FEW-NUCLEON SYSTEMS FOR NUCLEAR PHYSICS*

J. Golak, R. Skibiński, H. Witała, D. Ramirez
V. Urbanevych, V. Chahar

for the LENPIC Collaboration

M. Smoluchowski Institute of Physics, Jagiellonian University
30-348 Kraków, Poland

Received 28 November 2022, accepted 1 December 2022,
published online 22 March 2023

The chiral effective field theory (EFT) and *ab initio* few- and many-body methods play a very important role in precision nuclear theory. In this contribution, the current status of the chiral nuclear forces derived by the Low Energy Nuclear Physics International Collaboration (LENPIC) is discussed and the role of three-nucleon continuum calculations within LENPIC is described.

DOI:10.5506/APhysPolBSupp.16.4-A23

1. Introduction

The structure of the nuclear Hamiltonian is the central problem of nuclear physics. This Hamiltonian is dominated by pair-wise interactions, which can be studied already in two-nucleon systems. The necessity for the three-nucleon force (3NF) was realized when three-nucleon (3N) bound states were calculated exactly [1–3] using early nucleon–nucleon (NN) potentials [4–8], later replaced by semi-phenomenological NN potentials which described the NN data with high precision (χ^2/datum ≈ 1) [9–11]. Subsequent calculations of the four-nucleon (4N) bound state [12, 13] confirmed these findings and the observed underbinding of the 3N and 4N bound states was removed when the nuclear Hamiltonian was supplemented by a 3NF model, such as the Tucson–Melbourne (TM) [14] or the Urbana IX [15].

The bound states did not provide enough information about the properties of the 3N Hamiltonian and it became clear that 3N scattering observables were necessary to shed more light on this problem. It was thus very important that in the early 1990s numerical solutions of the 3N Faddeev equations for nucleon–deuteron scattering with the inclusion of realistic 3N

---

* Presented at the Zakopane Conference on Nuclear Physics, *Extremes of the Nuclear Landscape*, Zakopane, Poland, 28 August–4 September, 2022.

forces were prepared by Henryk Witała and collaborators. This achievement had a great impact on the field of few-nucleon physics and enabled many experimental groups to perform measurements sensitive to the structure of the 3N force. All essential results obtained before the mid-1990s for the 3N system were summarized in an important review paper [16].

The calculations of the elastic nucleon–deuteron scattering reaction and the nucleon-induced deuteron breakup process performed with the semi-phenomenological NN forces [9–11] revealed (see, for example, Refs. [16–18]) in general good agreement of theoretical predictions with data for 3N scattering observables at the incoming nucleon energies below approximately 30 MeV. At higher energies, however, the theoretical predictions based on NN forces only did not fully describe the data. For example, the agreement between theory and data in the minimum of the elastic scattering cross section was restored, when the 3NF models [14, 15] were additionally employed in the 3N calculations [17–20]. For many spin observables in elastic nucleon–deuteron scattering, none of the available combinations of 2N and 3N forces could describe the data, although the theory predicted large 3NF effects, see, for example, Refs. [18, 21]. The situation was not improved by the results obtained within the consistent relativistic framework [24, 25], because the cross sections and polarization observables were only slightly changed by including relativity [24, 25].

All these studies proved that the Tucson–Melbourne and Urbana IX 3NF models had severe limitations and a major step forward required 3NF models consistent with 2N potentials, containing also some number of short-range components with a richer spin structure. This could be realized only within the chiral effective field theory.

2. Nucleon–deuteron scattering with chiral nuclear potentials

Low-energy 3N scattering was investigated for the first time with chiral next-to-next-to-leading order (N2LO) 2N and 3N forces in [26]. Later, in Refs. [27, 28], 2N forces were derived at next-to-next-to-next-to-leading order (N3LO) of the chiral expansion and could be used in a wider energy range. It turned out that experimental phase-shifts were described by these potentials equally well as by the semi-phenomenological 2N forces [29, 30]. The N3LO contributions to the 3NF developed in Refs. [31, 32] do not contain any additional unknown parameters so the full N3LO 3NF possesses only two low-energy constants. In order to fix these parameters, usually the experimental triton binding energy and at least one 3N scattering observable are necessary. The latter could be, for example, the nucleon–deuteron doublet scattering length but recently, the very precise experimental data for the proton–deuteron differential cross section at the proton laboratory energy of 70 MeV from Ref. [23] is chosen.

The first-generation chiral 2N and 3N forces were tested in the calculations of the elastic nucleon–deuteron scattering observables [33]. It was found that non-local regularization applied directly in momentum space resulted in strong finite-cutoff artefacts in the predictions for higher energies, which precluded employing such forces in further 3N continuum calculations. This problem was solved in more recent generations of 2N chiral potentials prepared up to next-to-next-to-next-to-leading order (N4LO). While the first of them [34, 35] employed a local coordinate-space regularization of the one- and two-pion exchange contributions, the newest one from Ref. [36] uses a momentum-space version of the local regulator. In Ref. [37], the authors describe the key features of these semi-local momentum-space regularized (SMS) NN potentials and demonstrate their outstanding performance in the 2N sector. In particular, the SMS NN potentials of Ref. [36] at the highest available order (the so-called "N4LO$^+$") provide, for the regulator values $\Lambda = 450$ and 500 MeV, a nearly perfect description of mutually compatible neutron–proton and proton–proton scattering data below the laboratory nucleon energy $E_{\mathrm{lab}} = 300$ MeV with $\chi^2/\mathrm{datum} = 1.01$. This places these potentials among the most accurate and precise NN interactions to date.

A comparable level of precision beyond the NN sector is currently not achieved due to both computational limitations and unavailability of consistently regularized many-nucleon forces beyond the third order of the chiral EFT expansion. This problem is also addressed in Ref. [37]. The 2N and 3N potentials have to be regularized in order to obtain a well defined solution of the Faddeev equations. High-momentum components in the integrals appearing in the iterations of the Faddeev equation produce contributions with positive powers and logarithms of the cutoff parameter Λ, which diverge for $\Lambda \to \infty$ and are supposed to get absorbed by the available short-range interactions. The momentum dependence of such contact contributions in a 3N force is, however, severely constrained by the spontaneously broken chiral symmetry of QCD. This makes the consistent regularization of 2N and 3N potentials very difficult. The authors of Ref. [37] point to possible solutions to this problem but this goal has not been achieved yet.

In the meantime, a series of detailed investigations of low-energy three-nucleon scattering observables and selected properties of light and medium-mass nuclei at low orders in chiral EFT has been performed by the LENPIC Collaboration [38] using different variants of chiral EFT NN interactions [34–36] with and without the 3N force at N2LO [26, 39], see Refs. [40, 41, 43–45]. Some results calculated up to 2019 have been also reported in conference proceedings, see, for example, [46, 47]. These studies provide the explicit and implicit (that is based on the discrepancies between calculated observables and experimental data) verification of the 3NF effects, which are compatible with the expected size of N2LO corrections, in agreement with the Weinberg power counting [49, 50]. Additionally, the results give insights into the convergence pattern of chiral EFT for nuclear systems and implications for uncertainty quantification. In Ref. [45], selected nucleon–deuteron elastic scattering and breakup observables have been calculated. Further results have included properties of the $A = 3$ and $A = 4$ nuclei as well as spectra of p-shell nuclei up to $A = 16$ using the SMS potentials at leading, next-to-leading and N2LO from Ref. [36] in combination with the 3N force at N2LO regularized in the same way as the SMS NN potentials. While the obtained predictions at N2LO proved to be generally consistent with experimental data within errors, a systematic overbinding of nuclei was found starting from $A \approx 10$ and increasing with A. Moreover, a slight underprediction was observed for the ^{4}He structure radius, which however was still consistent with the experimental value at the 95% confidence level.

The main purpose of the most recent LENPIC paper [48] was to shed light on the origin of the significant (even at the 95% confidence level) overbinding of heavier p-shell nuclei at N2LO found in Ref. [45]. To clarify whether this discrepancy is related to deficiencies of the NN force at N2LO or rather has to be resolved by higher-order corrections to the 3NF, the authors have performed a series of calculations based on the higher-order SMS NN potentials (N3LO, N4LO, and N4LO$^+$) in combination with the 3NF at N2LO. While the obtained predictions are still accurate only at the N2LO level due to the missing contributions to the many-body forces at N3LO and beyond, the overbinding issue has been resolved by including higher-order contributions to the NN force. Furthermore, the results of Ref. [45] have been extended to heavier nuclei by performing calculations for the oxygen and calcium isotope chains and studying the convergence pattern of chiral EFT for the corresponding charge radii. Additionally, the large generated set of calculated energy levels has enabled the authors to perform a more detailed error analysis of the correlated excitation energies of the considered nuclei.

3. Neutron analyzing power in the deuteron breakup process

In the following, we give an example of a typical study in the 3N system and show an analysis of the sensitivity of the neutron analyzing power $A_y(n)$ to details of the chiral interaction. We choose the incident neutron energy of $E = 135$ MeV. Our predictions are obtained within the Faddeev scheme [16], using the SMS NN potential [36] at N2LO or N4LO$^+$, in both cases supplemented by the N2LO three-nucleon interaction [45]. We use regulator values $\Lambda = 400$, 450 or 550 MeV. By finding the transition amplitude for the breakup process, we are able to predict the nucleon analyzing power $A_y(n)$ at any kinematically allowed configuration. In the case of the three-body final state, such a configuration is unambiguously defined by five kinematical variables which we choose to be two pairs of angles (polar and azimuthal) corresponding to the momenta of the two outgoing neutrons $(\theta_1, \phi_1, \theta_2, \phi_2)$ and additionally a position (S) on the kinematical S-curve [16] which fixes energies of the two detected neutrons. We studied approximately five million kinematical configurations, what allows us to recognize at which configurations various aspects of chiral dynamics are important.

To illustrate this, we compute, for each point on a (θ_1, θ_2) grid, the differences

$$\begin{aligned} \delta^{400-550}(\theta_1, \theta_2, \phi_2, S) \;\equiv\; & (A_y(n))^{400}(\theta_1, \theta_2, \phi_2, S) \\ & -(A_y(n))^{550}(\theta_1, \theta_2, \phi_2, S) \end{aligned} \tag{1}$$

and

$$\begin{aligned} \delta^{\mathrm{N2LO-N4LO+}}(\theta_1, \theta_2, \phi_2, S) \;\equiv\; & (A_y(n))^{\mathrm{N2LO}}(\theta_1, \theta_2, \phi_2, S) \\ & -(A_y(n))^{\mathrm{N4LO+}}(\theta_1, \theta_2, \phi_2, S)\,, \end{aligned} \tag{2}$$

where the upper index of $A_y(n)$ shows which order of the NN interaction or which cut-off value is used. If not written explicitly, N4LO$^+$ or $\Lambda = 450$ MeV is applied. Note that in that study we restrict ourselves to $\phi_1 = 0^\circ$ (and thus skip ϕ_1 in the definitions above), but in general, a study of polarization observables can be extended also to $\phi_1 \neq 0^\circ$.

Next, we find, for given θ_1 and θ_2, maxima of $\delta^{400-550}(\theta_1, \theta_2, \phi_2, S)$ and $\delta^{\mathrm{N2LO-N4LO+}}(\theta_1, \theta_2, \phi_2, S)$ over two remaining variables (ϕ_2 and S), obtaining corresponding $\Delta(\theta_1, \theta_2)^{400-550}$ and $\Delta(\theta_1, \theta_2)^{\mathrm{N2LO-N4LO+}}$.

These two quantities are shown in Fig. 1. $\Delta(\theta_1, \theta_2)^{400-550}$ is small and changes from ≈ -0.10 up to ≈ 0.13. The dependence of $\Delta(\theta_1, \theta_2)^{400-550}$ on θ_1 and θ_2 is clearly seen — the highest values are present for the part of the phase space where $\theta_1 < 60^\circ$ and θ_2 lies within the range $(30^\circ, 150^\circ)$. In turn, for most configurations with θ_1 below approx. 60° and $\theta_1 < 140^\circ$, $(A_y(n))^{550}$ is smaller than $(A_y(n))^{400}$ which results in a negative $\Delta(\theta_1, \theta_2)^{400-550}$. In other parts of the phase space, $\Delta(\theta_1, \theta_2)^{400-550}$ remains of the order of a few percent demonstrating a small sensitivity of the neutron analyzing power to the cut-off value. In the case of $\Delta(\theta_1, \theta_2)^{\mathrm{N2LO-N4LO+}}$, we see two separate areas in the θ_1–θ_2 plane with relatively big positive values of $\Delta(\theta_1, \theta_2)^{\mathrm{N2LO-N4LO+}}$. These areas are adjacent to regions where $\Delta(\theta_1, \theta_2)^{\mathrm{N2LO-N4LO+}}$ is negative and smaller than -0.04. In other parts of the phase space both N2LO and N4LO$^+$ NN interactions, supplemented by the N2LO 3NF, lead to very similar predictions.

Having in mind the possible experimental verification of our predictions, in Fig. 2 we show again $\Delta(\theta_1, \theta_2)^{400-550}$ and $\Delta(\theta_1, \theta_2)^{\mathrm{N2LO-N4LO+}}$ but now obtained after imposing additional restrictions on the cross sections (≥ 0.01 [mb sr^{-2} MeV^{-1}]), the analyzing powers ($|A_y(n)| > 0.3$) and the kinetic energies of detected neutrons ($E \geq 10$ MeV). These conditions

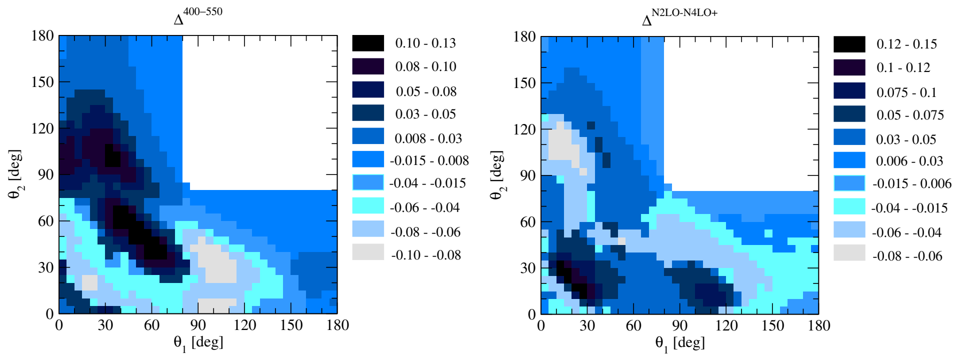

Fig. 1. $\Delta^{400-550}$ (left) and $\Delta^{\rm N2LO-N4LO+}$ (right) at the incoming nucleon laboratory kinetic energy $E_{\rm lab} = 135$ MeV. θ_1 and θ_2 are polar angles of two outgoing neutrons, calculated with respect to the initial beam. The kinematically forbidden areas in the θ_1–θ_2 plane are marked in white.

significantly reduce the number of allowed configurations, what is reflected in Fig. 2 by a large white area. However, the assumed restrictions do not affect basically the magnitudes of $\Delta(\theta_1,\theta_2)^{400-550}$ and $\Delta(\theta_1,\theta_2)^{\rm N2LO-N4LO+}$, which span the range between $(-0.06, 0.10)$ and $(-0.07, 0.09)$, respectively. In the case of the cut-off dependence of $A_y(n)$, the areas characterized by extreme values of $\Delta(\theta_1,\theta_2)^{400-550}$ are small and in the bulk of the phase space $(A_y(n))^{400} \approx (A_y(n))^{550}$. The $\Delta(\theta_1,\theta_2)^{\rm N2LO-N4LO+}$ behaves differently and takes values close to extremal in a big part of the allowed area. However, on the absolute scale, the $\Delta(\theta_1,\theta_2)^{\rm N2LO-N4LO+}$ remains small revealing only small differences between calculations based on the N2LO and N4LO+ NN interactions.

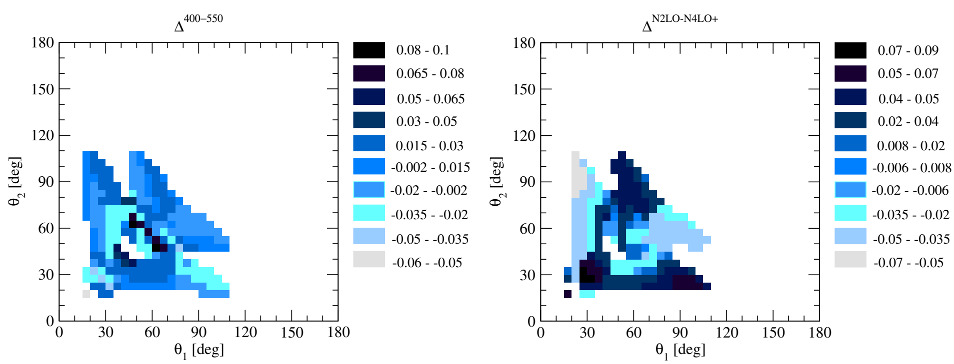

Fig. 2. $\Delta^{400-550}$ (left) $\Delta^{\rm N2LO-N4LO+}$ (right) at the incoming nucleon laboratory kinetic energy $\rm E_{lab} = 135$ MeV. Compared to Fig. 1, the additional thresholds for the energies of detected neutrons, the magnitude of the cross sections, and the magnitude of the analyzing powers $A_y(n)$ have been imposed (see the text for specific values).

In Fig. 3, we show predictions for two example configurations which contribute to Fig. 2. We give results from all the models used to build $\Delta^{400-550}$ and $\Delta^{\mathrm{N2LO-N4LO+}}$. For the configuration shown in the left panel of Fig. 3, in the maximum of $A_y(n)$ around $S = 80$ MeV, a change of the regulator value from $\Lambda = 400$ MeV to $\Lambda = 550$ MeV raises $(A_y(n))^{\mathrm{N4LO+}}$ by 0.068. We also see that increasing the chiral order of the two-nucleon component of the interaction from N2LO to N4LO+ decreases $A_y(n)$ by the same value of 0.068. The position of the black solid curve ($\Lambda = 450$ MeV) with respect to predictions obtained for $\Lambda = 400$ MeV and $\Lambda = 550$ MeV reveals more or less linear dependence of $A_y(n)$ on Λ for this configuration. In contrast, an example given in the right panel of Fig. 3 shows the case for which there is a strong sensitivity to the regulator value used, while the change of the order of the NN interaction has a much smaller impact on $A_y(n)$. In some other cases not shown in this contribution, for example, for the configuration specified by choosing $\theta_1 = 92.5°, \phi_1 = 0°, \theta_2 = 22.5°$, and $\phi_2 = 177.5°$, the cut-off effects and dependence on the chiral order of the NN force is similar for 50 MeV$< S <$ 120 MeV, leading to $|\Delta^{400-550}| \approx |\Delta^{\mathrm{N2LO-N4LO+}}| \approx 0.04$, but the nonlinear dependence of $A_y(n)$ on Λ is observed, as $(A_y(n))^{400} \approx (A_y(n))^{450} < (A_y(n))^{550}$. Moreover, at the minimum of $A_y(n)$ around $S = 145$ MeV all the N4LO+ based predictions overlap, while the N2LO results are greater by 0.07.

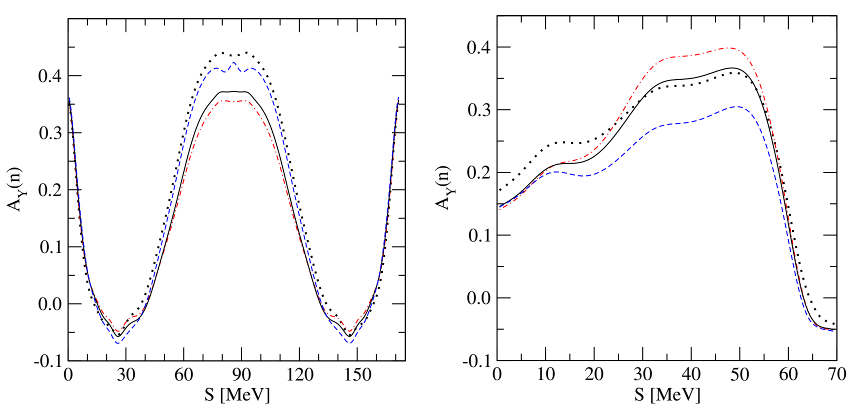

Fig. 3. (Color online) The neutron analyzing power $A_y(n)$ at the incoming nucleon laboratory kinetic energy $E_{\mathrm{lab}} = 135$ MeV for the configuration defined by $\theta_1 = 17.5°, \phi_1 = 0°, \theta_2 = 17.5°$, $\phi_2 = 2.5°$ (left) and by $\theta_1 = 47.5°, \phi_1 = 0°$, $\theta_2 = 62.5°$, $\phi_2 = 2.5°$ (right). Predictions based on the complete (NN+3NF) N2LO, $\Lambda = 450$ MeV interaction are represented by the black dotted curve. Predictions based on the N4LO$^+$ NN interaction supplemented with the N2LO 3N force with $\Lambda = 400$, 450, and 550 MeV are given by the red dash-dotted, black solid, and blue dashed curves, respectively.

The presented above example of a complex pattern of polarization observables related to the cut-off dependence and to the interaction model used, demonstrates the sensitivity of the deuteron breakup process to details of chiral dynamics. We are aware that the experimental investigations aimed at examining the results presented here are challenging but they are not impossible with the current experimental technology.

4. Summary

Theoretical investigations of three-nucleon systems have been performed by Henryk Witała and collaborators since the late 1980s. These studies are based on rigorous solutions of the 3N continuum Faddeev equations in momentum space for energies below the pion production threshold. The calculations involve description of cross sections and many polarization observables in elastic nucleon–deuteron scattering as well as in nucleon-induced deuteron breakup processes. The aim of these efforts has been always to understand the structure of nuclear forces and (later) the properties of the electroweak current operators. The investigations of the 3N force effects have been especially important and led to very intense collaboration with many experimental groups. Recently, we have concentrated on the forces derived within chiral EFT by the LENPIC Collaboration.

In particular, the most advanced SMS NN interactions have been recently used [48] to analyze 3N scattering observables and selected properties of light and medium-mass nuclei. To this end, Hamiltonians comprising higher-order nucleon–nucleon potentials in combination with the three-nucleon force at N2LO were first determined using the $A = 3$ binding energies and selected nucleon–deuteron cross sections as input. The Hamiltonians were then used to calculate other nucleon–deuteron scattering observables, spectra of light p-shell nuclei, and ground-state energies of nuclei in the oxygen isotopic chain from ^{14}O to ^{26}O as well as ^{40}Ca and ^{48}Ca. These new results give insights into the convergence pattern of chiral EFT for light- and medium-mass nuclei.

The accuracy of these studies is limited by the fact that the corresponding 3N force is only available at N2LO. At this chiral order, the predicted nucleon–deuteron scattering observables and ground-state energies of nuclei with $A \leq 12$ agree with the data within truncation error. Work on constructing consistent SMS 3N potentials beyond N2LO is in progress and will open an avenue for performing high-accuracy chiral EFT calculations beyond the 2N system.

Meanwhile, we show a typical for our Cracow group investigation of the neutron analyzing power $A_y(n)$ in the neutron-induced deuteron breakup reaction at the incident neutron energy of $E = 135$ MeV. The study gives information about various aspects of chiral dynamics.

This work is part of the LENPIC project and we thank other LENPIC members for sharing with us their expertise in the field of chiral forces discussed in this contribution. The numerical calculations were partially performed on the supercomputer cluster of the JSC, Jülich, Germany.

REFERENCES

[1] W. Glöckle, *Nucl. Phys. A* **381**, 343 (1982).
[2] T. Sasakawa, S. Ishikawa, *Few-Body Syst.* **1**, 3 (1986).
[3] A. Nogga *et al.*, *Phys. Rev. C* **67**, 034004 (2003).
[4] M.M. Nagels, T.A. Rijken, J.J. de Swart, *Phys. Rev. D* **17**, 768 (1978).
[5] M. Lacombe *et al.*, *Phys. Rev. C* **21**, 861 (1980).
[6] R.B. Wiringa, R.A. Smith, T.L. Ainsworth, *Phys. Rev. C* **29**, 1207 (1984).
[7] R. Machleidt, K. Holinde, Ch. Elster, *Phys. Rep.* **149**, 1 (1987).
[8] R. Machleidt, *Adv. Nucl. Phys.* **19**, 189 (1989).
[9] V.G.J. Stoks *et al.*, *Phys. Rev. C* **49**, 2950 (1994).
[10] R.B. Wiringa, V.G.J. Stoks, R. Schiavilla, *Phys. Rev. C* **51**, 38 (1995).
[11] R. Machleidt, *Phys. Rev. C* **63**, 024001 (2001).
[12] A. Nogga, H. Kamada, W. Glöckle, *Phys. Rev. Lett.* **85**, 944 (2000).
[13] A. Nogga *et al.*, *Phys. Rev. C* **65**, 054003 (2002).
[14] S.A. Coon *et al.*, *Nucl. Phys. A* **317**, 242 (1979).
[15] B.S. Pudliner *et al.*, *Phys. Rev. C* **56**, 1720 (1997).
[16] W. Glöckle *et al.*, *Phys. Rep.* **274**, 107 (1996).
[17] H. Witała *et al.*, *Phys. Rev. Lett.* **81**, 1183 (1998).
[18] H. Witała *et al.*, *Phys. Rev. C* **63**, 024007 (2001).
[19] R.V. Cadman *et al.*, *Phys. Rev. Lett.* **86**, 967 (2001).
[20] B.v. Przewoski *et al.*, *Phys. Rev. C* **74**, 064003 (2006).
[21] R. Bieber *et al.*, *Phys. Rev. Lett.* **84**, 606 (2000).
[22] H. Shimizu *et al.*, *Nucl. Phys. A* **382**, 242 (1982).
[23] K. Sekiguchi *et al.*, *Phys. Rev. C* **65**, 034003 (2002).
[24] H. Witała *et al.*, *Phys. Rev. C* **71**, 054001 (2005).
[25] H. Witała *et al.*, *Phys. Rev. C* **77**, 034004 (2008).
[26] E. Epelbaum *et al.*, *Phys. Rev. C* **66**, 064001 (2002).
[27] D.R. Entem, R. Machleidt, *Phys. Rev. C* **68**, 041001 (2003).
[28] E. Epelbaum, W. Glöckle, U.-G. Meißner, *Nucl. Phys. A* **747**, 362 (2005).
[29] J.R. Bergervoet *et al.*, *Phys. Rev. C* **41**, 1435 (1990).
[30] V.G.J. Stoks *et al.*, *Phys. Rev. C* **48**, 792 (1993).
[31] V. Bernard *et al.*, *Phys. Rev. C* **77**, 064004 (2008).
[32] V. Bernard *et al.*, *Phys. Rev. C* **84**, 054001 (2011).

[33] H. Witała *et al.*, *J. Phys. G: Nucl. Part. Phys.* **41**, 094011 (2014).

[34] E. Epelbaum, H. Krebs, U.-G. Meißner, *Eur. Phys. J. A* **51**, 53 (2015).

[35] E. Epelbaum, H. Krebs, U.-G. Meißner, *Phys. Rev. Lett.* **115**, 122301 (2015).

[36] P. Reinert, H. Krebs, E. Epelbaum, *Eur. Phys. J. A* **54**, 86 (2018).

[37] E. Epelbaum, H. Krebs, P. Reinert in: I. Tanihata, H. Toki, T. Kajino (Eds.) «Handbook of Nuclear Physics», *Springer*, 2022, `arXiv:2206.07072 [nucl-th]`.

[38] The LENPIC website, `http://www.lenpic.org/`

[39] U. van Kolck, *Phys. Rev. C* **49**, 2932 (1994).

[40] LENPIC Collaboration (S. Binder *et al.*), *Phys. Rev. C* **93**, 044002 (2016).

[41] LENPIC Collaboration (S. Binder *et al.*), *Phys. Rev. C* **98**, 014002 (2018).

[42] H. Witała *et al.*, *Few-Body Syst.* **57**, 1213 (2016).

[43] LENPIC Collaboration (E. Epelbaum *et al.*), *Phys. Rev. C* **99**, 024313 (2019).

[44] E. Epelbaum *et al.*, *Eur. Phys. J. A* **56**, 92 (2020).

[45] LENPIC Collaboration (P. Maris *et al.*), *Phys. Rev. C* **103**, 054001 (2021).

[46] J. Golak *et al.*, *SciPost Phys. Proc.* **3**, 002 (2020).

[47] J. Golak *et al.*, *Acta Phys. Pol. B Proc. Suppl.* **13**, 609 (2020).

[48] LENPIC Collaboration (P. Maris *et al.*), *Phys. Rev. C* **106**, 064002 (2022), `arXiv:2206.13303 [nucl-th]`.

[49] S. Weinberg, *Phys. Lett. B* **251**, 288 (1990).

[50] S. Weinberg, *Nucl. Phys. B* **363**, 3 (1991).